

Properties of Bose Gases with Raman-Induced Spin-Orbit Coupling

Wei Zheng¹, Zeng-Qiang Yu^{1,2}, Xiaoling Cui¹ and Hui Zhai¹

¹ Institute for Advanced Study, Tsinghua University, Beijing, 100084, China.

² Dipartimento di Fisica, Università di Trento and INO-CNR BEC Center, I-38123 Povo, Italy.

Abstract. In this paper we investigate the properties of Bose gases with Raman-induced spin-orbit(SO) coupling. It is found that the SO coupling can greatly modify the single particle density-of-state, and thus lead to non-monotonic behavior of the condensate depletion, the Lee-Huang-Yang correction of ground-state energy and the transition temperature of a non-interacting Bose-Einstein condensate. The presence of the SO coupling also breaks the Galilean invariance, and this gives two different critical velocities, corresponding to the movement of the condensate and the impurity respectively. Finally, we show that with SO coupling, the interactions modify the BEC transition temperature even at Hartree-Fock level, in contrast to the ordinary Bose gas without SO coupling. All results presented here can be directly verified in the current cold atom experiments using Raman laser-induced gauge field.

1. Introduction

Recently one of the major progresses in cold atom physics is the realization of spin-orbit (SO) coupling for neutral atoms with the idea of light induced synthetic gauge field [1, 2, 3, 4]. Previously, effects of spin-orbit coupling have only been studied in fermionic matters such as electron gases, while this progress opens up the new opportunity of studying SO coupling in bosonic systems. This investment is interesting because SO coupling changes many basic properties of Bose-Einstein condensation (BEC) in both quantitative and qualitative way.

Although SO coupling emerges at single particle level, it may have a significant effect to the many-body behavior due to the modification of the single particle density-of-state (DoS). One particular example is the Rashba SO coupled Bose gases. Because of the dramatic change of low energy DoS, many intriguing many-body phenomena have been predicted there, and some questions still have not been thoroughly understood yet. While a number of theoretical works have studied its low-temperature properties, including ground state phases, quantum and thermal fluctuations, Bose condensation transition and superfluidity [5, 6, 7, 8, 9, 10, 11], the experimental realization of Rashba SO coupling remains to be a great challenge. On the other hand, the type of equal Rashba and Dresselhaus SO coupling has been realized in current experiment with two photon Raman transition. Although the change of low-energy DoS is not as dramatic as Rashba case, such a SO coupling leads to a non-monotonic behavior of low-energy DoS as a function of Raman strength, which should result in nontrivial manifestation of many-body properties. So far, a few papers have studied the ground state phase diagram, collective modes and response function for such SO coupled condensate [12, 13, 14, 15, 16, 17], but there are still several fundamental properties which have not been explored, in particular, the depletion of the condensate, the BEC transition temperature and the superfluid critical velocities. In this work we report our theoretical studies of these properties.

2. Single particle Hamiltonian and mean-field phase diagram

2.1. Single particle Hamiltonian

In current experiments, two counter-propagating Raman beams are applied to couple two hyperfine levels of an alkali atom [1, 2, 3, 4], which gives rise to the single-particle Hamiltonian as [18] (set $\hbar = 1$)

$$\hat{H}_0 = \begin{pmatrix} (\hat{\mathbf{p}} - k_r \mathbf{e}_x)^2 / 2m + \delta/2 & \Omega/2 \\ \Omega/2 & (\hat{\mathbf{p}} + k_r \mathbf{e}_x)^2 / 2m - \delta/2 \end{pmatrix} \quad (1)$$

where k_r is the recoil momentum, Ω is the Raman coupling strength, and δ is the two-photon detuning. With Pauli matrix, the Hamiltonian in Eq. (1) can be rewritten as

$$\hat{H}_0 = \frac{\hat{\mathbf{p}}^2}{2m} - \mathbf{B}_{\mathbf{p}} \cdot \boldsymbol{\sigma} + E_r \quad (2)$$

where $E_r = k_r^2/(2m)$ is the recoil energy, and $\mathbf{B}_{\mathbf{p}} = (-\Omega/2, 0, k_r p_x/m - \delta/2)$ depends on momentum p_x and yields the locking between spin and momentum. This Hamiltonian preserves spatial translational symmetry, and momentum \mathbf{p} is a good quantum number. Another quantum number of this Hamiltonian is "helicity" $h = \pm$,

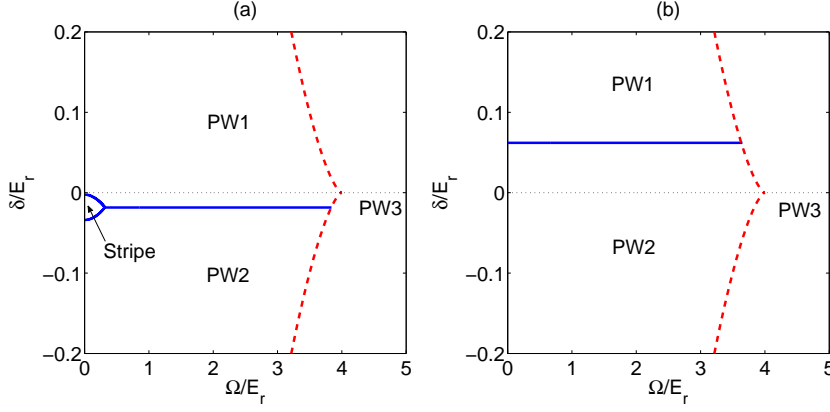


Figure 1. The phase diagrams of ^{87}Rb (a) and ^{23}Na (b). The two pseudo-spin states are $m = 0, -1$ states of $F = 1$ hyperfine states. On the right of red dashed line, the single particle spectrum has one local minimum, and there is only one plane wave phase (PW3). On the left of red dashed line, the single particle spectrum has two local minima, and the horizontal blue line separates two plane-wave condensates at different momenta (PW1 and PW2). Within the region rounded by two blues lines it is the stripe phase, in which the condensate coherently occupies two different momenta. Here $E_r = 2\pi \times 2.2\text{kHz}$.

which denotes for $\mathbf{B}_{\mathbf{p}}$ parallel or anti-parallel to spin σ . Thus, the eigen-energies of two helicity branches are given by

$$\varepsilon_{\mathbf{p},\pm} = \frac{p^2}{2m} + \frac{k_r^2}{2m} \pm \sqrt{\left(\frac{p_x k_r}{m} - \frac{\delta}{2}\right)^2 + \left(\frac{\Omega}{2}\right)^2} \quad (3)$$

and their wave-functions are given by

$$\phi_{\mathbf{p},+}(\mathbf{r}) = e^{i\mathbf{p}\cdot\mathbf{r}} \begin{pmatrix} \sin \theta_{\mathbf{p}} \\ \cos \theta_{\mathbf{p}} \end{pmatrix}; \quad \phi_{\mathbf{p},-}(\mathbf{r}) = e^{i\mathbf{p}\cdot\mathbf{r}} \begin{pmatrix} \cos \theta_{\mathbf{p}} \\ -\sin \theta_{\mathbf{p}} \end{pmatrix} \quad (4)$$

with

$$\theta_{\mathbf{p}} = \arcsin \left[\frac{1}{2} \left(1 + \frac{p_x k_r / m - \delta / 2}{\sqrt{(p_x k_r / m - \delta / 2)^2 + \Omega^2 / 4}} \right) \right]^{1/2}$$

With the spectrum, the single particle DoS can be calculated straightforwardly as

$$D(\epsilon) = \frac{1}{V} \sum_{\mathbf{p}} [\delta_D(\epsilon - \varepsilon_{\mathbf{p},+}) + \delta_D(\epsilon - \varepsilon_{\mathbf{p},-})] \quad (5)$$

where δ_D is Dirac delta function.

2.2. Mean-field phase diagram

The interaction of a two-component Bose gas is generally written as

$$\hat{H}_I = \frac{1}{2} \int d^3\mathbf{r} \left(g_{\uparrow\uparrow} \hat{\psi}_{\uparrow}^{\dagger} \hat{\psi}_{\uparrow}^{\dagger} \hat{\psi}_{\uparrow} \hat{\psi}_{\uparrow} + g_{\downarrow\downarrow} \hat{\psi}_{\downarrow}^{\dagger} \hat{\psi}_{\downarrow}^{\dagger} \hat{\psi}_{\downarrow} \hat{\psi}_{\downarrow} + 2g_{\uparrow\downarrow} \hat{\psi}_{\uparrow}^{\dagger} \hat{\psi}_{\downarrow}^{\dagger} \hat{\psi}_{\downarrow} \hat{\psi}_{\uparrow} \right). \quad (6)$$

With mean-field approximation, the interaction energy is given by

$$\mathcal{E}_I = \frac{1}{2} \int d^3\mathbf{r} (g_{\uparrow\uparrow} n_{\uparrow}^2(\mathbf{r}) + g_{\downarrow\downarrow} n_{\downarrow}^2(\mathbf{r}) + 2g_{\uparrow\downarrow} n_{\uparrow}(\mathbf{r}) n_{\downarrow}(\mathbf{r})) \quad (7)$$

When δ and Ω are both small, ϵ_- has two local minima located at \mathbf{k}_{\pm} . Without loss of generality, we can assume the condensate wave function as

$$\varphi(\mathbf{r}) = \sqrt{n_0} \left[\cos \alpha \begin{pmatrix} \cos \theta_+ \\ -\sin \theta_+ \end{pmatrix} e^{i\mathbf{p}_+ \cdot \mathbf{r}} + \sin \alpha \begin{pmatrix} \sin \theta_- \\ -\cos \theta_- \end{pmatrix} e^{i\mathbf{p}_- \cdot \mathbf{r}} \right], \quad (8)$$

where $0 \leq \alpha \leq \pi/2$, $\cos \alpha$ and $\sin \alpha$ are superposition coefficients. It gives

$$\begin{aligned} n_{\uparrow} &= n_0 [\cos^2 \alpha \cos^2 \theta_+ + \sin^2 \alpha \cos^2 \theta_- + \sin 2\alpha \cos \theta_+ \cos \theta_- \cos(\delta \mathbf{p} \cdot \mathbf{r})], \\ n_{\downarrow} &= n_0 [\cos^2 \alpha \sin^2 \theta_+ + \sin^2 \alpha \sin^2 \theta_- + \sin 2\alpha \sin \theta_+ \sin \theta_- \cos(\delta \mathbf{p} \cdot \mathbf{r})] \end{aligned} \quad (9)$$

where $\delta \mathbf{p} = \mathbf{p}_+ - \mathbf{p}_-$. In practices, one can straightforwardly substitute the expression of density Eq. 9 into the interaction energy Eq. 7, and the interaction energy \mathcal{E}_I becomes a function of α , \mathbf{p}_{\pm} and θ_{\pm} . Then by minimizing the total energy respect to α , \mathbf{p}_{\pm} and θ_{\pm} , one can finally obtain the ground state condensate wave function for given Ω , δ and interaction parameters $g_{\uparrow\uparrow}$, $g_{\downarrow\downarrow}$ and $g_{\uparrow\downarrow}$. Thus, a phase diagram can be constructed. More details have been discussed in Ref. [1, 12, 13] and here we will just emphasize some general features.

(1) If the energy minimization gives $\alpha = 0$ or $\alpha = \pi/2$, there is only one momentum component in the condensate wave function, and the density for both spin component are uniform, as it can be easily seen by setting $\alpha = 0$ or $\pi/2$ in Eq. (9). This is the “plane wave” condensate. While if the energy minimization gives $0 < \alpha < \pi/2$, both $n_{\uparrow}(\mathbf{r})$ and $n_{\downarrow}(\mathbf{r})$ have spatially periodic modulation. This is named as “stripe” condensate [5].

(2) Because of SO coupling, the densities of both components depend on momentum. If the interaction is $SU(2)$ invariant, i.e. $g_{\uparrow\uparrow} = g_{\downarrow\downarrow} = g_{\uparrow\downarrow} = g$, the interaction energy becomes $\mathcal{E}_I = (g/2) \int d^3\mathbf{r} (n_{\uparrow}(\mathbf{r}) + n_{\downarrow}(\mathbf{r}))^2$. In this case, if the condensate is in the “plane wave” phase, the interaction energy is independent of momentum, and one can take \mathbf{p}_{\pm} as \mathbf{k}_{\pm} which minimizes the single particle energy. However, because the two pseudo-spin states are taken as two hyperfine level of atoms, they do not have to obey $SU(2)$ spin rotational symmetry. Thus, for a general case, three interaction parameters $g_{\uparrow\uparrow}$, $g_{\downarrow\downarrow}$ and $g_{\uparrow\downarrow}$ are all unequal. Therefore, even for the plane wave condensate, the interaction energy also depends on momentum p_{\pm} . That is equivalent to say, even at mean-field level the self-energy correction has momentum dependence, which effectively modifies the single particle dispersion and changes the location of its minimum. In contrast, without SO coupling, the mean-field self-energy correction is just a constant shift of single particle energy. Thus, as first pointed out by Ref. [13], \mathbf{p}_{\pm} is shifted away from single particle minimum \mathbf{k}_{\pm} ‡.

(3) The stripe phase has distinct properties from plane-wave phase. For the stripe phase, the total density will have spatial modulation, because the spin wave function at \mathbf{p}_+ and \mathbf{p}_- are not orthogonal, i.e., $\cos \theta_{\mathbf{p}_+} \cos \theta_{\mathbf{p}_-} + \sin \theta_{\mathbf{p}_+} \sin \theta_{\mathbf{p}_-} \neq 0$ §. Thus, in this system the stripe phase is not favored by density interaction part $(g/2) \int d^3\mathbf{r} (n_{\uparrow}(\mathbf{r}) + n_{\downarrow}(\mathbf{r}))^2$. In another word, if the interaction is $SU(2)$ invariant,

‡ However, for some special case, such as pure Rashba SO coupling without Zeeman field considered in Ref. [5], the mean-field self-energy correlation is also momentum independent.

§ This is also different from pure Rashba case where the spin wave function are orthogonal for opposite momentum, and the total density is uniform for stripe phase

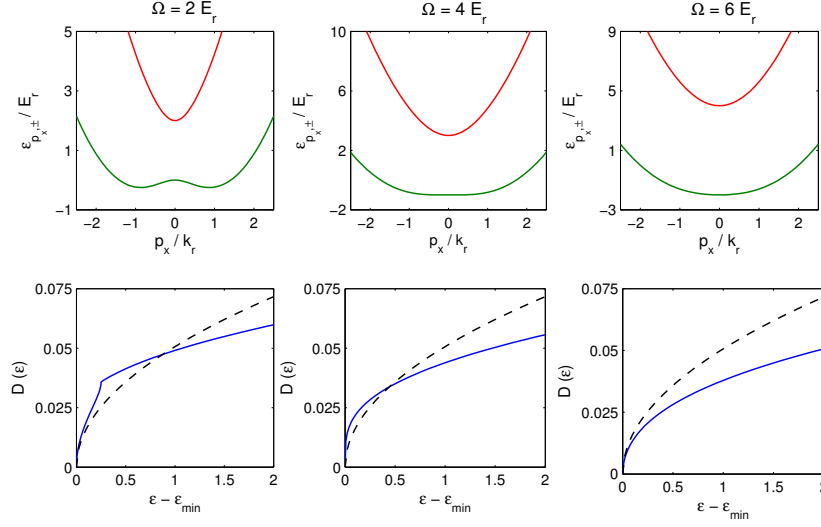


Figure 2. Upper panel: Single particle dispersion $\epsilon_{\pm}(p_x)$ as a function of p_x/k_r ; Lower panel: DoS as a function of $\epsilon - \epsilon_{\min}$ for $\Omega = 2E_r$, $4E_r$ and $6E_r$, respectively. ϵ_{\min} denotes the minimum value of single particle energy. The dashed lines are DoS for the case without Raman coupling.

stripe phase will not exist in this system. The difference in $g_{\uparrow\uparrow}$, $g_{\downarrow\downarrow}$ and $g_{\uparrow\downarrow}$ are necessary for stabilizing the stripe phase. Moreover, since the non-uniform term in total density increases as Ω increases. Thus, the stripe phase, if exists, should be found in small Ω regime of the phase diagram.

(4) Consider the limit $\Omega = 0$, if $g_{\uparrow\uparrow}g_{\downarrow\downarrow} - g_{\uparrow\downarrow}^2 > 0$, a homogeneous mixture of two components is stable against local density fluctuations, and there will be a mixed phase within certain detuning window. Such a mixed phase will turn into stripe phase once Ω becomes non-zero, for instance, for ^{87}Rb case in Fig. 1(a). While if $g_{\uparrow\uparrow}g_{\downarrow\downarrow} - g_{\uparrow\downarrow}^2 < 0$, the mixed phase is not stable against phase separation even for zero Ω , and there will be no stripe phase in the phase diagram, for instance, for ^{23}Na case in Fig. 1(b).

Hereafter, we should focus only on $SU(2)$ invariant interaction. This is relevant for experiment with Rb or Na, because the difference in $g_{\uparrow\uparrow}$, $g_{\downarrow\downarrow}$ and $g_{\uparrow\downarrow}$ are smaller than 1%. The generalization to non- $SU(2)$ interaction is straightforward. Besides, we only consider the plane wave phase, because in these systems, the stripe phase either occupies a very small regime of phase diagram or does not exist.

2.3. Zero-detuning case

In this work we will particularly focus on the case with $\delta = 0$ for following two reasons.

(1) *Density-of-State Effect.* When $\Omega < 4E_r$, $\epsilon_{\pm}(k_x)$ has two minima at $k_{\pm} = \pm k_r \sqrt{1 - \left(\frac{\Omega}{4E_r}\right)^2}$, and when $\Omega > 4E_r$, $\epsilon_{\pm}(k_x)$ has one single minimum at $k_x = 0$. Expanding the dispersion around its minimum, one gets the effective mass in x

direction as

$$m^* = \begin{cases} m \left(1 - \frac{\Omega^2}{16E_r^2}\right)^{-1} & \Omega < 4E_r \\ m \left(1 - \frac{4E_r}{\Omega}\right)^{-1} & \Omega > 4E_r \end{cases}. \quad (10)$$

Hence, the low-energy DoS increases with Ω when $\Omega < 4E_r$ and decreases with Ω when $\Omega > 4E_r$, as shown in Fig. 2. The most intriguing point is at $\Omega = 4E_r$ when the single particle dispersion behaves as $\sim p_x^4$ at the lowest order and the low-energy DoS reaches its maximum. As we shall see in later discussion, this has important physical consequences in the superfluid critical velocity and the BEC transition temperature.

(2) *Z₂ Symmetry and Magnetization.* When $\Omega < 4E_r$, bosons condense into one of the minima, which breaks the Z_2 symmetry. The Bose condensate will have finite magnetization. While when $\Omega > 4E_r$, bosons condense at zero-momentum state and the condensate is non-magnetic. Thus, there will be a magnetic phase transition at $\Omega = 4E_r$ associated with the Z_2 symmetry breaking, and a divergent spin susceptibility has been predicted and experimentally found [4, 15]. We note that such a transition exists only for $\delta = 0$, since for non-zero δ the Hamiltonian does not possess the Z_2 symmetry, and the condensate phase is always magnetic.

3. Bogoliubov Theory and Superfluid Critical Velocity

3.1. Bogoliubov Spectrum

We study the fluctuations around the condensate with Bogoliubov theory. Considering a plane-wave condensate at momentum $\mathbf{p}_0 = p_0 \mathbf{e}_x$, the field operator can be expanded as

$$\hat{\psi}(\mathbf{r}) = \varphi(\mathbf{r}) + \delta\hat{\psi}(\mathbf{r}) \quad (11)$$

where $\varphi(\mathbf{r})$ is the condensate wave-function

$$\varphi(\mathbf{r}) = \sqrt{n_0} \begin{pmatrix} \cos \theta_{p_0} \\ -\sin \theta_{p_0} \end{pmatrix} \exp(ip_0 x) \quad (12)$$

and satisfies the Gross-Pitaevskii (GP) equation

$$\left[H_0(p_0) + gn_0 \mathbf{I} \right] \begin{pmatrix} \cos \theta_{p_0} \\ -\sin \theta_{p_0} \end{pmatrix} = \mu \begin{pmatrix} \cos \theta_{p_0} \\ -\sin \theta_{p_0} \end{pmatrix}. \quad (13)$$

Defining $\hat{\Psi}_{\mathbf{q}}^\dagger = (\psi_{\mathbf{p}_0+\mathbf{q},\uparrow}^\dagger, \psi_{\mathbf{p}_0+\mathbf{q},\downarrow}^\dagger, \psi_{\mathbf{p}_0-\mathbf{q},\uparrow}, \psi_{\mathbf{p}_0-\mathbf{q},\downarrow})$, the Bogoliubov Hamiltonian for the fluctuation part can be written as

$$\mathcal{K} = \sum_{q_x > 0} \hat{\Psi}_{\mathbf{q}}^\dagger \mathcal{K}_{\mathbf{q}} \hat{\Psi}_{\mathbf{q}} - \frac{1}{2} \sum_{q_x > 0} [\epsilon_{\mathbf{p}_0-\mathbf{q},\uparrow} + \epsilon_{\mathbf{p}_0-\mathbf{q},\downarrow} - 2\mu + 3gn_0]$$

where

$$\mathcal{K}_{\mathbf{q}} = \begin{pmatrix} K_0(\mathbf{p}_0 + \mathbf{q}) + \Sigma_N & \Sigma_A \\ \Sigma_A & K_0(\mathbf{p}_0 - \mathbf{q}) + \Sigma_N \end{pmatrix} \quad (14)$$

$K_0 = H_0 - \mu$ is the grand Hamiltonian of non-interacting system, Σ_N and Σ_A are normal and anomalous self-energy respectively

$$\Sigma_N = gn_0 \begin{pmatrix} \sin^2 \theta_{p_0} + 2 \cos^2 \theta_{p_0} & -\sin \theta_{p_0} \cos \theta_{p_0} \\ -\sin \theta_{p_0} \cos \theta_{p_0} & \cos^2 \theta_{p_0} + 2 \sin^2 \theta_{p_0} \end{pmatrix}; \quad (15)$$

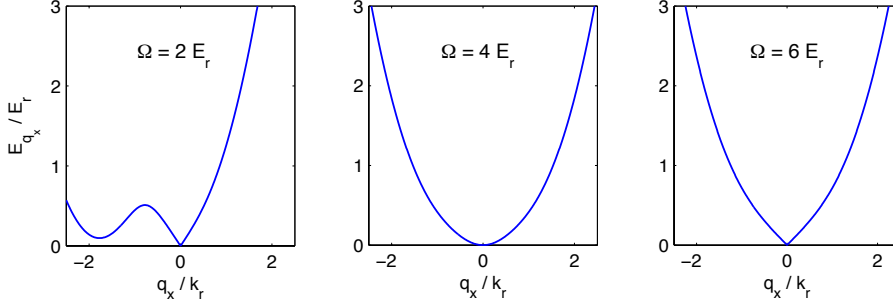


Figure 3. Bogoliubov spectrum for $\Omega/E_r = 2, 4$ and 6 for (a-c). gn/E_r is fixed to be 0.5 .

$$\Sigma_A = gn_0 \begin{pmatrix} \cos^2 \theta_{p_0} & -\sin \theta_{p_0} \cos \theta_{p_0} \\ -\sin \theta_{p_0} \cos \theta_{p_0} & \sin^2 \theta_{p_0} \end{pmatrix}. \quad (16)$$

Hence the Bogoliubov spectrum is determined by

$$\text{Det} \begin{pmatrix} K_0(\mathbf{p}_0 + \mathbf{q}) + \Sigma_N - E & \Sigma_A \\ -\Sigma_A & -K_0(\mathbf{p}_0 - \mathbf{q}) - \Sigma_N - E \end{pmatrix} = 0 \quad (17)$$

Because of the emergence of off-diagonal long range order, the excitation energy should be gapless in the long wave-length limit $\mathbf{q} \rightarrow 0$, which requires

$$\text{Det} \left[\Sigma_A (K_0(p_0) + \Sigma_N)^{-1} \Sigma_A - (K_0(p_0) + \Sigma_N) \right] = 0 \quad (18)$$

This equation is indeed satisfied because GP equation for the condensate wave-function can be rewritten as

$$\text{Det} \left[H_0(p_0) - \mu + \Sigma_N - \Sigma_A \right] = 0 \quad (19)$$

Eq. (19) can also be regarded as a generalization of Hugenholtz-Pines relation $\mu = \Sigma_N - \Sigma_A$ to the SO coupled Bose gases [19].

Solving Eq. (17) gives rise to the entire Bogoliubov spectrum $E_{\mathbf{q},\pm}$. Examples are displayed in Fig. 3 for various Ω/E_r . For $\mathbf{q}_x \rightarrow 0$, the low-energy excitation is the phonon mode with a linear dispersion $E_-(q_x) = sq_x$. Along the direction of Raman beam, the sound velocity is given by

$$s = \sqrt{\frac{gn_0}{m} \left(1 - \frac{\Omega^2}{16E_r^2} \right)} \quad (20)$$

when $\Omega < 4E_r$ and

$$s = \sqrt{\frac{gn_0}{m} \left(1 - \frac{4E_r}{\Omega} \right)} \quad (21)$$

when $\Omega > 4E_r$. These results are consistent with the effective mass approximation that gives $s = \sqrt{gn_0/m^*}$. At $\Omega = 4E_r$, the effective mass diverges, and the low-energy phonon mode is quadratic in q_x^2 , as shown in Fig. 3(b). This is a significant difference compared to the conventional phonon mode, which is always linear in \mathbf{q} . When $\Omega < 4E_r$, the Bogoliubov spectrum has another local minimum at finite q_x , which is due to the double degeneracy in single particle spectrum. This is attributed as “roton minimum” by Ref. [15].

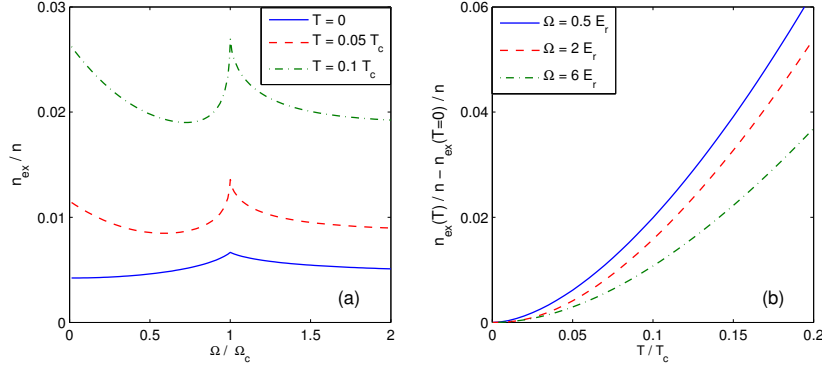


Figure 4. (a) Total depletion as a function of Ω/E_r for $T = 0, 0.05T_c$ and $0.1T_c$, where T_c is the condensation temperature (see Section 4). (b) Thermal depletion as a function of T/T_c for various values of Ω/E_r (take $gn/E_r = 0.5$ and $n/k_r^3 = 1$).

3.2. Quantum and Thermal Condensate Depletion

The Bogoliubov Hamiltonian can be straightforwardly written as

$$\begin{aligned} \mathcal{K}^{(2)} = & \sum_{\mathbf{q} \neq 0} (E_{\mathbf{q},+} \hat{\psi}_{\mathbf{q},+}^{\dagger} \hat{\psi}_{\mathbf{q},+} + E_{\mathbf{q},-} \hat{\psi}_{\mathbf{q},-}^{\dagger} \hat{\psi}_{\mathbf{q},-}) \\ & + \frac{1}{2} \sum_{\mathbf{q} \neq 0} [E_{-\mathbf{q},+} + E_{-\mathbf{q},-} - \epsilon_{\mathbf{p}_0-\mathbf{q},\uparrow} - \epsilon_{\mathbf{p}_0-\mathbf{q},\downarrow} + 2\mu - 3gn_0] \end{aligned} \quad (22)$$

here $\hat{\Psi}_{\mathbf{q}}^{\dagger} \equiv (\hat{\psi}_{\mathbf{q},+}^{\dagger}, \hat{\psi}_{\mathbf{q},-}^{\dagger}, \hat{\psi}_{-\mathbf{q},+}, \hat{\psi}_{-\mathbf{q},-}) = M_{\mathbf{q}}^{-1} \hat{\Psi}_{\mathbf{q}}$ are quasi-particle operators, and $M_{\mathbf{q}}$ is the Bogoliubov transformation matrix which is obtained from eigen equation (17). The quantum and thermal depletion of condensate $n_{\text{ex},\sigma} = \frac{1}{V} \sum_{\mathbf{q} \neq 0} \langle \hat{\psi}_{\mathbf{p}_0+\mathbf{q},\sigma}^{\dagger} \hat{\psi}_{\mathbf{p}_0+\mathbf{q},\sigma} \rangle$ thus can be readily calculated using $M_{\mathbf{q}}$ and $E_{\mathbf{q},\pm}$.

The depletion fraction as a function of Raman coupling strength Ω and temperature T is shown in Fig. 4. The contribution to depletion is mainly from two parts: the low-energy phonon part and the roton part. At zero-temperature, the contribution is dominated by the phonon part because the roton part has a finite excitation gap. Thus, due to the non-monotonic behavior of sound velocity discussed above, when $\Omega < 4E_r$, the quantum depletion n_{ex}/n increases with Ω , reaches a maximum at $\Omega = 4E_r$, and then decreases as Ω increases. At finite temperature, because the roton gap is quite small at small Ω , the roton part will give an significant contribution. For $\Omega < 4E_r$, the contribution from phonon part always increases with Ω because the decrease of phonon velocity, while the contribution from roton part decreases with Ω because the roton gap increases with Ω . Due to the interplay of these two contributions, for small Ω , n_{ex}/n first decreases as Ω increase, in contrast to zero-temperature case. Then n_{ex}/n increases again with Ω and the peak of n_{ex}/n at $\Omega = 4E_r$ retains.

Another interesting manifestation of roton minimum is through the magnetization of non-condensed part defined as $(n_{\text{ex}\uparrow} - n_{\text{ex}\downarrow})/n_{\text{ex}}$. Assuming the condensate momentum $p_0 > 0$, the condensate has a positive magnetization $(n_{0\uparrow} - n_{0\downarrow})/n_0 > 0$. As shown in Fig. 5 (a), at zero-temperature, the depletion also has a positive

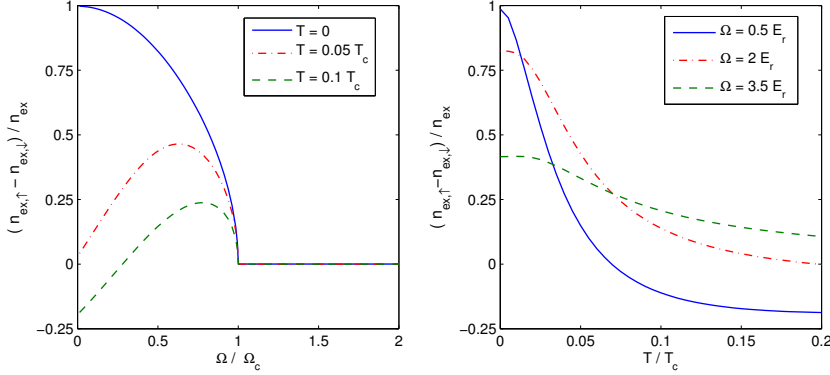


Figure 5. (a) Magnetization of depletion $(n_{\text{ex}\uparrow} - n_{\text{ex}\downarrow})/n_{\text{ex}}$ as a function of Ω/E_r for various temperatures. (b) $(n_{\text{ex}\uparrow} - n_{\text{ex}\downarrow})/n_{\text{ex}}$ as a function of T/T_c for various Ω . (parameters are the same as in Fig. 4)

magnetization $(n_{\text{ex}\uparrow} - n_{\text{ex}\downarrow})/n_{\text{ex}} > 0$. This is because the phonon contribution, which dominates the quantum depletion, originates from states whose momenta are nearby condensate momentum and possess same magnetization as the condensate. However, at finite temperature, for small Ω , the depletion can have opposite magnetizations as the condensate part, as shown in Fig. 5(a). And from Fig. 5(b) one can also see that, for instance at $\Omega = 0.5 E_r$, the magnetization soon decreases to negative as temperature increases. This is because the roton contribution dominates in this regime. Recall that when $\Omega < 4 E_r$ there is double minimum in this single particle spectrum with opposite momentum and magnetization. When condensate takes place in one of the minimum, the roton minimum in the excitation appears nearby the other minimum. Thus, the contribution from roton minimum displays opposite magnetization with condensate part. As we know, the phonon dispersion is linear, while the roton dispersion is quadratic. That implies the DoS of the quasi-particle near the roton is larger than the one near the phonon part. At finite temperatures higher than the roton gap, the thermal depletion near the roton minimum will exceed the depletion from phonon modes. This leads to an opposite magnetization of the total thermal depletion compared with the condensate. In the further experiment, measuring the magnetization of the thermal depletion will thus provide an evidence for the existence of the roton minimum in the excitation spectrum.

3.3. Beyond-mean-field correction of ground state energy

Bogoliubov theory also gives rise to a correction to mean-field energy usually named as Lee-Huang-Yang correction [20]. The Lee-Huang-Yang correction can be considered as a sum of all zero-point energies of excitation modes at different momenta. Without SO coupling, it is a function of $n^{1/3} a_s$ only and the ratio between energy correction to mean-field energy is

$$\frac{\mathcal{E}_{\text{LHY}}}{\mathcal{E}_{\text{MF}}} = \Gamma_{\text{LHY}}(n^{1/3} a_s) = \frac{128}{15\sqrt{\pi}} \sqrt{n a_s^3}. \quad (23)$$

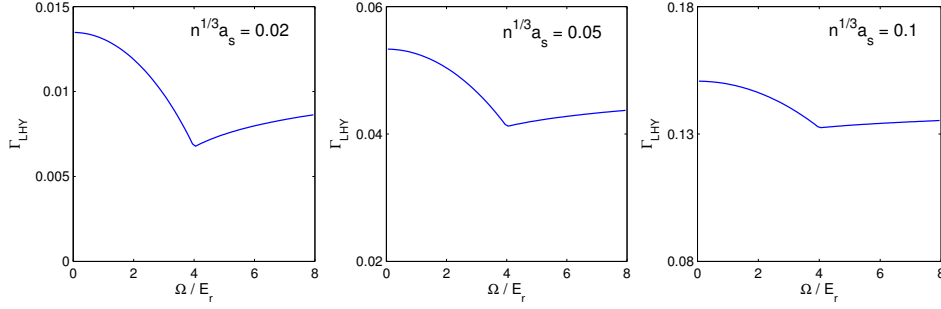


Figure 6. Γ_{LHY} as a function of Ω/E_r for different $n^{1/3}a_s$ (fixed $n/k_r^3 = 1$).

While with SO coupling, using Eq. (22) one finds that \mathcal{E}_{LHY} is given by

$$\begin{aligned} \mathcal{E}_{\text{LHY}} = & \frac{1}{2} \sum_{\mathbf{q} \neq 0} \left[E_{-\mathbf{q},+} + E_{-\mathbf{q},-} - \epsilon_{\mathbf{p}_0-\mathbf{q},\uparrow} - \epsilon_{\mathbf{p}_0-\mathbf{q},\downarrow} + 2\mu - \frac{12\pi a_s n}{m} \right] \\ & + \frac{8\pi^2 a_s^2 n^2}{m} \sum_{\mathbf{k}} \frac{1}{k^2} \end{aligned} \quad (24)$$

where the last term is obtained from the renormalization relation of coupling constant g via second-order Bohn approximation

$$g = \frac{4\pi a_s}{m} + \frac{(4\pi a_s)^2}{mV} \sum_{\mathbf{k}} \frac{1}{k^2} \quad (25)$$

Therefore Γ_{LHY} is a function of $n^{1/3}a_s$, Ω/E_r and n/k_r^3 , and the results are shown in Fig. 6. We find that the Lee-Huang-Yang correction shows a nonmonotonic behavior as a function of Raman coupling strength and displays a minimum at $\Omega_c = 4E_r$. This is consistent with the softening of phonon mode at Ω_c discussed above. The softer the phonon mode is, the smaller the zero-point energy will be, which results in the minimum in Lee-Huang-Yang correction.

3.4. Superfluid Critical Velocity

There are two ways to measure critical velocity [11]. First, the condensate is at rest and an impurity moves with finite velocity in the condensate. In this way, one can obtain a critical dragging velocity

$$\mathbf{v}_{\text{drag}} = \min \left(\frac{E_{\mathbf{q}}}{\mathbf{q}} \right), \quad (26)$$

where $E_{\mathbf{q}}$ is the quasi-particle energy for momentum \mathbf{q} . Critical dragging velocity is shown in Fig. 6(a). One can see that \mathbf{v}_{drag} vanishes at $4E_r$, because the phonon spectrum becomes quadratic in q_x at this point and the phonon velocity vanishes. One can also see that for $\Omega < 4E_r$, \mathbf{v}_{drag} is not symmetric for moving along \hat{x} or along $-\hat{x}$. This is due to the non-symmetric structure of Bogoliubov spectrum as shown in Fig. 3(a). Moving along \hat{x} , \mathbf{v}_{drag} is determined by phonon part. Moving along $-\hat{x}$, \mathbf{v}_{drag} is determined by the roton minimum for small Ω . Since the roton gap increases with Ω , the \mathbf{v}_{drag} along $-\hat{x}$ also increase with Ω until the roton vanishes. After that

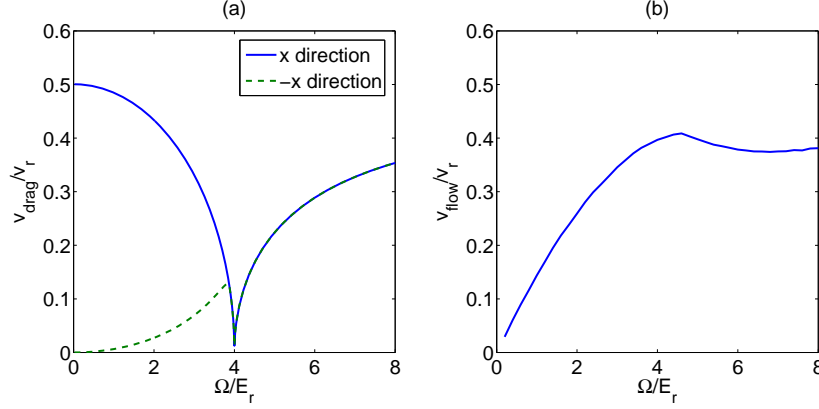


Figure 7. Critical dragging(a) and flowing(b) velocity as a function of Ω/E_r . Here $gn = 0.5E_r$, and $v_r = k_r/m$.

the \mathbf{v}_{drag} along $-\hat{x}$ is also determined by the phonon mode, and will decrease with Ω until $\Omega = 4E_r$.

Second, one can consider a static impurity and let the condensate move with a finite velocity. This determines another critical velocity which can be called critical flowing velocity \mathbf{v}_{flow} . If the system is Galilean invariant, \mathbf{v}_{drag} and \mathbf{v}_{flow} should be identical. However, SO coupling breaks the Galilean invariance, and thus these two velocities become unequal, as first pointed out in Ref. [11] for Rashba type SO coupling. In our system, Galilean invariance is also broken. Considering a Galilean transformation in \hat{x} direction, the Hamiltonian in the moving frame becomes

$$H_0(\mathbf{v}) = \frac{1}{2m} \left\{ (\hat{p}_x - k_r \sigma_z)^2 \right\} + \frac{1}{2} \Omega \sigma_x - v_x p_x \quad (27)$$

$$= \frac{1}{2m} [\hat{p}_x - (k_r \sigma_z + m v_x)]^2 + \frac{1}{2} \Omega \sigma_x - v_x k_r \sigma_z - \frac{1}{2} m v^2 \quad (28)$$

With a gauge transformation $U(\mathbf{x}, t) = \exp[-i m v_x x - i (m v^2/2) t]$, the Hamiltonian becomes

$$H_0(\mathbf{v}) = \frac{1}{2m} (\hat{p}_x - k_r \sigma_z)^2 + \frac{1}{2} \Omega \sigma_x - v_x k_r \sigma_z \quad (29)$$

Compared to the Hamiltonian in the stationary frame, there is an additional velocity dependent Zeeman term $v_x k_r \sigma_z$. This term can not be gauged away, and that implies the broken of Galilean invariance for a SO coupled particle. The physical effect of this term has already been observed in Ref. [4] in collective dipole oscillation experiment. $\mathbf{v}_{\text{flow}} \neq \mathbf{v}_{\text{drag}}$ is another manifestation of the absence of Galilean invariance.

To determine \mathbf{v}_{flow} we shall first find out the ground state wave function for the Hamiltonian in the comoving frame [Eq. (28)], say

$$\varphi'(\mathbf{x}) = \sqrt{n_0} \begin{pmatrix} \cos \theta' \\ -\sin \theta' \end{pmatrix} \exp(i \mathbf{p}'_0 \cdot \mathbf{x}). \quad (30)$$

Then, following similar procedure discussed above, one can find out the Bogoliubov spectrum above this new ground state in the comoving frame, denoted by $E'_{\mathbf{q}}(\mathbf{v})$.

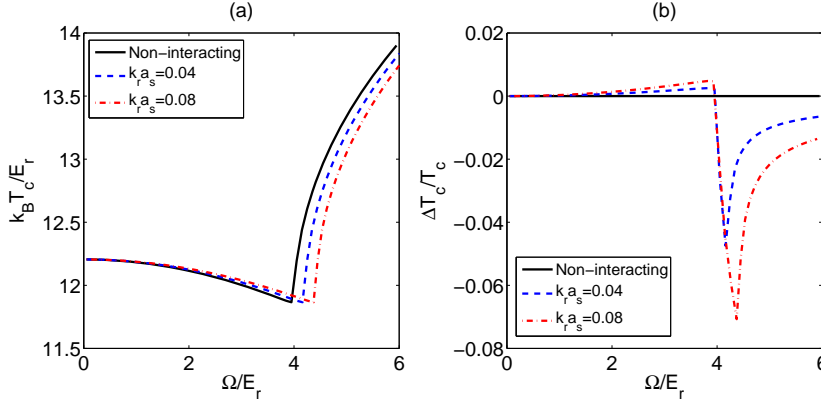


Figure 8. T_c (a) and its relative shift from non-interacting Bose gases $\Delta T_c / T_c$ (b) of a uniform system as a function of Ω / E_r for various interaction strengths. Here $n / k_r^3 = 5$.

Then, observing in the laboratory frame, the excitation spectrum is given by $E_{\mathbf{q}}(\mathbf{v}) = E'_{\mathbf{q}}(\mathbf{v}) + \mathbf{v} \cdot \mathbf{q}$. When \mathbf{v} is above certain critical value, $E_{\mathbf{q}}$ will start to have negative part, which indicates instability of the condensate. This critical values defines \mathbf{v}_{flow} . \mathbf{v}_{flow} of this system is shown in Fig. 7(b). We find that, strongly in contrast to \mathbf{v}_{drag} , \mathbf{v}_{flow} remains finite across $\Omega = 4E_r$. This is because in the comoving frame with finite velocity, the single particle spectrum is always quadratic around its minimum due to the velocity dependent Zeeman term, which prevents the softening of phonon mode.

4. Hartree-Fock theory of normal state and BEC transition temperature

4.1. Transition temperature of a noninteracting gas

Now we study the normal state of the system and determine the transition temperature of condensate. First, we consider a noninteracting gas. The condensation transition temperature T_c of a uniform system is given by (set $k_B = 1$)

$$n = \int_{-\infty}^{\infty} d\varepsilon \frac{D(\varepsilon)}{e^{(\varepsilon - \mu)/T_c} - 1}, \quad (31)$$

where chemical potential reaches the bottom of the single particle spectrum, $\mu = \epsilon_{\min}$. Due to the DoS effect discussed in Section 1, T_c decreases with Ω in the regime $\Omega < 4E_r$, reaches a minimum of finite value around $\Omega = 4E_r$, and then increase in the regime $\Omega > 4E_r$. This non-monotonic behavior is shown in Fig. 8(a). In $\Omega \rightarrow 0$ limit and $\Omega \rightarrow \infty$ limit, one can find a simple relation of transition temperature,

$$\frac{T_c(\Omega \rightarrow \infty)}{T_c(\Omega \rightarrow 0)} = 2^{2/3} \quad (32)$$

because the low-energy DoS for the later case shrinks to only half of the first one.

In a harmonic trap, the semiclassical energy of single boson can be expressed as

$$\varepsilon_{\mathbf{p},\pm}(\mathbf{r}) = \frac{1}{2m} (\mathbf{p}^2 + k_r^2) \pm \sqrt{(k_r p_x / m)^2 + \Omega^2 / 4} + \frac{1}{2} m \omega^2 r^2, \quad (33)$$

with ω the trap frequency. With semiclassical approximation, the DoS should be modified as

$$D_{\text{trap}}(\varepsilon) = \frac{1}{V} \sum_{\mathbf{p}} \int d^3r \left[\delta_D(\varepsilon - \varepsilon_{\mathbf{p},+}(\mathbf{r})) + \delta_D(\varepsilon - \varepsilon_{\mathbf{p},-}(\mathbf{r})) \right] \quad (34)$$

and the transition temperature can be obtained from

$$N = \int_{-\infty}^{\infty} d\varepsilon \frac{D_{\text{trap}}(\varepsilon)}{e^{(\varepsilon-\mu)/T_c} - 1} \quad (35)$$

when chemical potential μ reaches the minimum of single-particle energy at trap center. The result is shown in Fig. 9(a).

In contrast to uniform case, one finds the minimum location of the T_c is shifted into smaller Ω regime even for a small particle number. While if the particle number is large enough, T_c will always monotonically increases with Ω . This is because the effective mass increases with Ω , in a semiclassical sense it will leads an increasing of centre density in the trap of the thermal gas[22], $n_T(0) \propto (m^*T)^{3/2}$. From a quantum view of point, the effective harmonic length $a_{\text{ho}}^2 = \frac{\hbar}{\sqrt{m^*m\omega}}$ of the SO coupled Boson decrease with Ω . That also indicates the increasing of the central density. The density effect competes with DoS effects, and for large N the former dominates over the latter. In $\Omega \rightarrow \infty$ limit, due to the fact that DoS shrinks to one half of that in $\Omega \rightarrow 0$ limit, the transition temperature in these two regimes follows,

$$\frac{T_c(\Omega \rightarrow \infty)}{T_c(\Omega \rightarrow 0)} = 2^{1/3}. \quad (36)$$

4.2. Mean-field Shift of Transition Temperature for Uniform Gases

In the absence of SO coupling, it is well known that the contact interaction between the particles does not affect T_c at mean-field level [21], this is because the Hatree-Fock self-energy only provides a constant shift of chemical potential. While with SO coupling, as shown in the following, the interactions do have a non-trivial effect even at mean-field level.

To construct a self-consistent Hartree-Fock theory, besides the average density for each spin component

$$n_{\sigma} = \frac{1}{V} \sum_{\mathbf{p}} \langle \hat{\psi}_{\mathbf{p},\sigma}^{\dagger} \hat{\psi}_{\mathbf{p},\sigma} \rangle,$$

we also need to introduce mean-field parameter associating with the spin-flip term

$$\xi = \frac{1}{V} \sum_{\mathbf{p}} \langle \hat{\psi}_{\mathbf{p},\uparrow}^{\dagger} \hat{\psi}_{\mathbf{p},\downarrow} \rangle$$

The spin-flip term, ξ , is due to the Raman coupling between different spin states, which breaks the conservation of spin magnetization. In contrast, such a term is absent for an ordinary spinor Bose gas without Raman coupling.

Up to a constant, the mean-field Hamiltonian in Hartree-Fock approximation is given by

$$\begin{aligned} \hat{H}_{\text{HF}} = \hat{H}_0 + \sum_{\mathbf{p}} \left[g(2n_{\uparrow} + n_{\downarrow}) \hat{\psi}_{\mathbf{p},\uparrow}^{\dagger} \hat{\psi}_{\mathbf{p},\uparrow} + g(2n_{\downarrow} + n_{\uparrow}) \hat{\psi}_{\mathbf{p},\downarrow}^{\dagger} \hat{\psi}_{\mathbf{p},\downarrow} \right. \\ \left. + g\xi \left(\hat{\psi}_{\mathbf{p},\uparrow}^{\dagger} \hat{\psi}_{\mathbf{p},\downarrow} + \hat{\psi}_{\mathbf{p},\downarrow}^{\dagger} \hat{\psi}_{\mathbf{p},\uparrow} \right) \right] \end{aligned} \quad (37)$$

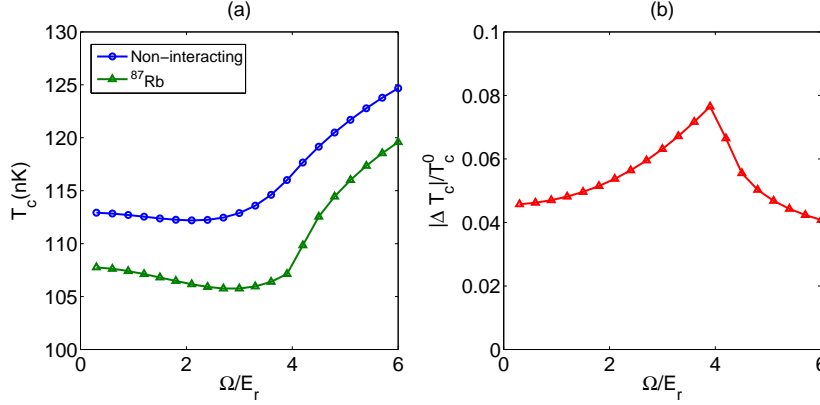


Figure 9. (a) T_c of ^{87}Rb and non-interacting Bose gases in the harmonic trap. (b) Shift of T_c of ^{87}Rb due to interaction as a function of Ω/E_r . Here $E_r = 2\pi \times 2.2\text{kHz}$. The particle number is $N = 2.5 \times 10^5$, and the trapping frequency is $\omega = 2\pi \times 50\text{Hz}$.

Since we are treating the normal state above T_c , spin are always unpolarized with $n_\uparrow = n_\downarrow = n/2$. The mean field Hamiltonian in (37) has the same structure as the single particle Hamiltonian, except that the Raman coupling is modified as $\Omega_{\text{eff}} = \Omega + 2g\xi$ and the energy zero-point is shifted by a constant. In this sense, we can define two dressed helicity branches, with dispersions given by

$$\varepsilon_{\mathbf{p},\pm} = \frac{1}{2m} (\mathbf{p}^2 + k_r^2) + \frac{3}{2}gn \pm \sqrt{(k_r p_x/m)^2 + \Omega_{\text{eff}}^2/4} \quad (38)$$

Here the mean-field parameter ξ should be solved self-consistently in combination with

$$\xi = \frac{1}{V} \sum_{\mathbf{p}} \sin \theta_{\mathbf{p}} \cos \theta_{\mathbf{p}} (n_{\mathbf{p},+} - n_{\mathbf{p},-}) \quad (39)$$

where $\theta_{\mathbf{p}}$ is given by Eq. (2.1) with the bare Raman coupling replaced by Ω_{eff} , and $n_{\mathbf{p},\pm}$ are Bose distribution functions with the dispersion $\varepsilon_{\mathbf{p},\pm}$ given by Eq. (38). The transition temperature T_c is then determined by interaction modified dispersions. Due to the non-trivial momentum-dependence of dispersions (38), the interactions induce a shift of T_c from non-interacting Bose gas.

Since the occupation of lower helicity branch $n_{\mathbf{p},-}$ is always larger than $n_{\mathbf{p},+}$, ξ is always negative and hence the effective Raman coupling strength Ω_{eff} is decreased to a smaller value. Based on the non-monotonic behavior of non-interacting T_c discussed previously, the minimum of the condensation temperature is shifted by the interaction to a larger Ω , as shown in Fig. 8 (a). Near the minimum, the correction of T_c change its sign rapidly within a narrow region of Ω/E_r . From Fig. 8(b), one can clearly see that the transition temperature is enhanced for $\Omega \lesssim 4E_r$ and is suppressed for $\Omega \gtrsim 4E_r$, and in between the correction $\Delta T_c = T_c - T_c^0$ shows a most profound effect around the T_c minimum.

4.3. Interaction Shift of Transition Temperature for Trapped Gases

Finally we come to discuss the most realistic case where both interaction and trap effect are taken into account. We use the Hatree-Fock mean-field theory to include interaction effect and use the semi-classical approximation to include trap effect.

Within the Hatree-Fock and semi-classical approximation, T_c is determined when $\mu(T)$ reaches the minimum of single particle spectrum, and $\mu(T)$ is determined by particle number conservation

$$N = \int d^3r n(\mathbf{r}, T, \mu) \quad (40)$$

Here the local density $n(\mathbf{r}, T, \mu)$ is given by

$$n(\mathbf{r}) = \int \frac{d^3k}{(2\pi)^3} \left\{ \frac{1}{e^{[\varepsilon_{+, \mathbf{k}}(\mathbf{r}) - \mu]/T} - 1} + \frac{1}{e^{[\varepsilon_{-, \mathbf{k}}(\mathbf{r}) - \mu]/T} - 1} \right\} \quad (41)$$

in which

$$\varepsilon_{\pm, \mathbf{k}}(\mathbf{r}) = \frac{1}{2m} (\mathbf{k}^2 + k_r^2) \pm \sqrt{(k_r k_x/m)^2 + \Omega_{\text{eff}}^2(\mathbf{r})/4 + V_{\text{eff}}(\mathbf{r})}, \quad (42)$$

and

$$V_{\text{eff}}(\mathbf{r}) = V(\mathbf{r}) + (3/2)gn(\mathbf{r}). \quad (43)$$

Similar as above, Ω_{eff} is the renormalized coupling as

$$\Omega_{\text{eff}}(\mathbf{r}) = \Omega + 2g\xi(\mathbf{r}). \quad (44)$$

which also needs to be determined self-consistently as Eq.39.

The numerical solution gives the interaction shift of T_c inside a harmonic trap, as shown in Fig. 9. Here we notice that the interaction effect always gives a negative shift of ΔT_c , in contrast to the uniform case where ΔT_c can be either positive or negative. This is because the presence of the repulsive interaction reduces the central density in the trap, leading to a reduced T_c . This effect dominates over the shift of Ω_{eff} for sufficient large particle number. In Fig. 9 we also plot $|\Delta T_c|/T_c^0$ as a function of Ω_c , and find the relative shift of T_c reaches a maximum around $\Omega = 4E_r$. This can be qualitatively understood from the effective mass approximation. Using m^* , one can define an effective scattering length $a_s^* = a_s(m^*/m)$ and harmonic length $a_{\text{ho}}^* = a_{\text{ho}}(m/m^*)^{1/4}$; therefore the shift of T_c in the harmonic trap[23] is $\Delta T_c/T_c^0 = -1.32 \frac{a_s^*}{a_{\text{ho}}^*} N^{1/6} \propto (m^*/m)^{5/4}$. As we have shown in Eq.10, m^*/m is maximally enhanced at $\Omega = 4E_r$, so the interaction has the maximum effect to the shift of T_c at this point.

5. Conclusion

In this paper, we investigate the properties of Bose gases with Raman-induced spin-orbit coupling. Our main results are summarized as follows.

(1) The presence of the SO coupling modifies the single particle spectrum and thus the single particle DoS. At $\Omega = 4E_r$, the low energy DoS reaches a maximum and the effective mass is maximally enhanced. The direct consequences include the vanishment of sound velocity at $\Omega = 4E_r$, and the non-monotonic behavior of condensate depletion, Lee-Huang-Yang correction of ground-state energy, and the transition temperature of a non-interacting Bose-Einstein condensate.

(2) The presence of the SO coupling breaks the Galilean invariance. As a result, the critical dragging and flowing velocity, respectively defined in the rest frame of the condensate and the impurity, are no longer identical.

(3) In the presence of the SO coupling, a roton minimum will appear in the excitation spectrum in the regime of $\Omega < 4E_r$. As a result, the thermal depletion of the condensate can possess an opposite magnetization with the quantum depletion. Moreover, the critical dragging velocity exhibits asymmetry along different directions.

(4) In the presence of the SO coupling, the interactions shift BEC transition temperature T_c even at a Hartree-Fock level. In both homogeneous and trapped systems, the interaction shift of T_c shows maximum around $\Omega = 4E_r$, where the interactions take the largest effect due to the enhancement of DoS and the effective mass.

In conclusion, we have shown that the Bose gases with Raman-induced SO coupling can exhibit a number of non-trivial properties, as summarized above. The results revealed here can be directly verified in the current cold atom experiments using laser-induced gauge field.

References

- [1] Lin Y.-J., Jiménez-García K. and Spielman I. B., *Nature*, **471** (2011) 83.
- [2] Wang P., Yu Z.-Q., Fu Z., Miao J., Huang L., Chai S., Zhai H. and Zhang J., *Phys. Rev. Lett.*, **109** (2012) 095301.
- [3] Cheuk L. W., Sommer A. T., Hadzibabic Z., Yefsah T., Bakr W. S. and Zwierlein M. W., *Phys. Rev. Lett.*, **109** (2012) 095302.
- [4] Zhang J.-Y., Ji S.-C., Chen Z., Zhang L., Du Z.-D., Yan B., Pan G.-S., Zhao B., Deng Y.-J., Zhai H., Chen S., and Pan J.-W., *Phys. Rev. Lett.* **109** (2012) 115301.
- [5] Wang C., Gao C., Jian C.-M., and Zhai H., *Phys. Rev. Lett.* **105**, (2010) 160403.
- [6] Stanescu T. D., Anderson B., and Galitski V., *Phys. Rev. A* **78**, 023616 (2008).
- [7] Wu C. J. and Mondragon-Shem I., *Chin. Phys. Lett.* (28)(9), (2011) 097102.
- [8] Ozawa T. and Baym G., *Phys. Rev. Lett.* **109** (2012) 025301; Ozawa T. and Baym G., arXiv:1203.6367.
- [9] Cui X. and Zhou Q., arXiv:1206.5918.
- [10] Zhou Q. and Cui X., arXiv:1210.5853.
- [11] Zhu Q., Zhang C. and Wu B., *Europhys. Lett.*, **100** (2012) 50003.
- [12] Ho T.-L. and Zhang S., *Phys. Rev. Lett.*, **107** (2011) 150403.
- [13] Li Y., Pitaevskii L. P. and Stringari S., *Phys. Rev. Lett.*, **108** (2012) 225301.
- [14] Li Y., Martone G. L. and Stringari S., *Europhys. Lett.*, **99** (2012) 56008.
- [15] Martone G. L., Li Y., Pitaevskii L. P. and Stringari S., *Phys. Rev. A*, **86** (2012) 063621.
- [16] Chen Z. and Zhai H., *Phys. Rev. A* **86** (2012) 041604(R).
- [17] Zheng W. and Li Z., *Phys. Rev. A* **85** (2012) 053607.
- [18] Zhai H., *Int. J. Mod. Phys. B*, **26**, 1230001 (2012).
- [19] Hugenholtz, N. and Pines, D. *Phys. Rev.* (1959) **116**, 489.
- [20] Lee T. D., Huang K., and Yang C. N., *Phys. Rev.* **106** (1957) 1135.
- [21] Fetter A. L. and Walecka J. D., *Quantum Theory of Many-Particle System*, Dover, 1971.
- [22] Pitaevskii L. P. and Stringari S., *Bose-Einstein Condensation*, Oxford, 2003.
- [23] Giorgini S., Pitaevskii L. P. and Stringari S., *Phys. Rev. A* **54** (1996) 4633.